Normal-Incidence Electrostatic Rydberg Atom Mirror

E. Vliegen and F. Merkt

Laboratorium für Physikalische Chemie, ETH Zürich CH-8093, Zurich, Switzerland

(Received 27 March 2006; published 19 July 2006)

A Rydberg atom mirror has been designed and its operational principle tested experimentally. A supersonic expansion containing H atoms moving with a velocity of 720 m/s initially propagates toward a quadrupolar electrostatic mirror. The H atoms are then photoexcited to $n = 27$ Rydberg states with a positive Stark shift and move in a rapidly increasing electric field. The H atom beam is stopped in 4.8 μs, only 1.9 mm away from the photoexcitation spot, and is then reflected back. The reflection process is monitored by pulsed field ionization and imaging.

DOI: 10.1103/PhysRevLett.97.033002 PACS numbers: 32.60.+i, 32.80.Rm, 34.60.+z, 39.90.+d

A growing number of experimental tools are becoming available to manipulate the translational motion of atoms and molecules in the gas phase and to investigate the properties of ultracold atoms and molecules [1,2] with important applications in several subfields of physics and chemistry such as reaction dynamics, metrology [3], and quantum information technology [4]. So far, experimental work has been focused on the manipulation of the velocity distribution of particles in their ground state or in low-lying metastable electronic states. Only isolated attempts have been made to manipulate the translational motion of electronically excited particles. The properties of Rydberg states [5], however, are ideally suited to the requirements of atom and molecule optics experiments: high Rydberg states respond strongly to electromagnetic fields and open up the possibility of realizing new devices such as atomic and molecular mirrors, lenses, and traps [6,7]. Schemes for accelerating [8] and trapping [9] Rydberg atoms using inhomogeneous electric fields were proposed more than 20 years ago and rely on the large dipole moments that arise in Rydberg states as a result of the linear Stark effect. Recently, these ideas have been exploited to build the first devices enabling control of the translational motion of Rydberg atoms [Kr [10], Ar [11–13], and H [14]] and molecules [H_2 [15,16]].

We report here on the first experimental realization of a normal-incidence Rydberg atom mirror. Its operational principle relies on the large force exerted on Rydberg particles by inhomogeneous electric fields as a result of the linear Stark effect. This force $\vec{f}$ can be expressed in atomic units as:

$$\vec{f} = -\tfrac{3}{2} n k \nabla F, \tag{1}$$

where n is the principal quantum number, k is a quantum number which labels the Stark states and runs from $-(n - 1 - |m|)$ to $(n - 1 - |m|)$ in steps of 2, and F is the electric field strength in atomic units. Inhomogeneous fields that can routinely be applied in the laboratory suffice to obtain accelerations of up to 10^8 m/s^2 [14]. The small mass of H and the fact that the crossings between Stark states are traversed diabatically when H Rydberg atoms move in an inhomogeneous electric field [14] make samples of H Rydberg atoms particularly attractive for atom optics experiments. The electrostatic mirror developed here can in principle be used to reflect a wider range of particles because all atoms and molecules have Rydberg states. Applications of the present Rydberg atom mirror in atom and molecule interferometry and in ultrahigh-resolution measurements of the energy intervals between highly excited electronic states may be envisaged. The normal-incidence H atom mirror presented here may also help prevent the antihydrogen Rydberg atoms generated at CERN [17] from colliding with the walls of the experimental chamber and annihilating there.

H atoms in a cold, pulsed supersonic expansion are generated by the 193 nm excimer photolysis of NH_3 in a 10:1 Ar:NH_3 gas mixture in a quartz capillary located at the exit of a pulsed solenoid valve. The skimmed gas expansion is intersected at right angles by counterpropagating vuv and uv laser beams and the H atoms are excited to Rydberg Stark states in a resonant two-photon excitation process via the $2\,^2P$ state [14]. Photoexcitation takes place in the middle of the four metallic plates of the electrostatic mirror depicted in Fig. 1(b). The figure also shows [panel (a)] the voltage pulse sequence used to reflect and field ionize the H Rydberg atoms. This sequence consists of three phases: photoexcitation [$t = 0$, voltage configuration in panel (b)], mirroring [500 ns $< t < t_{\text{ion}}$, panel (c)], and field ionization [$t = t_{\text{ion}}$, panel (d)].

The atoms are excited to the $n = 27$, $k = 18$, $|m| = 0, 2$ Stark states in the field generated by applying voltages $V_1 = -V_2 = 45$ V to the two plates on the nozzle side of the mirror [Fig. 1(b)]. 500 ns after photoexcitation, a first voltage pulse $V_4 = -V_3 = 700$ V of adjustable duration τ and of 50 ns rise time is applied to the plates on the detector side of the mirror [Fig. 1(c)]. This voltage pulse reverses the sign of the z component of the electric field vector within the mirror. During the sign reversal the electric field strength returns to exactly zero in the middle ($y = 0$) plane of the mirror, potentially causing a loss of the

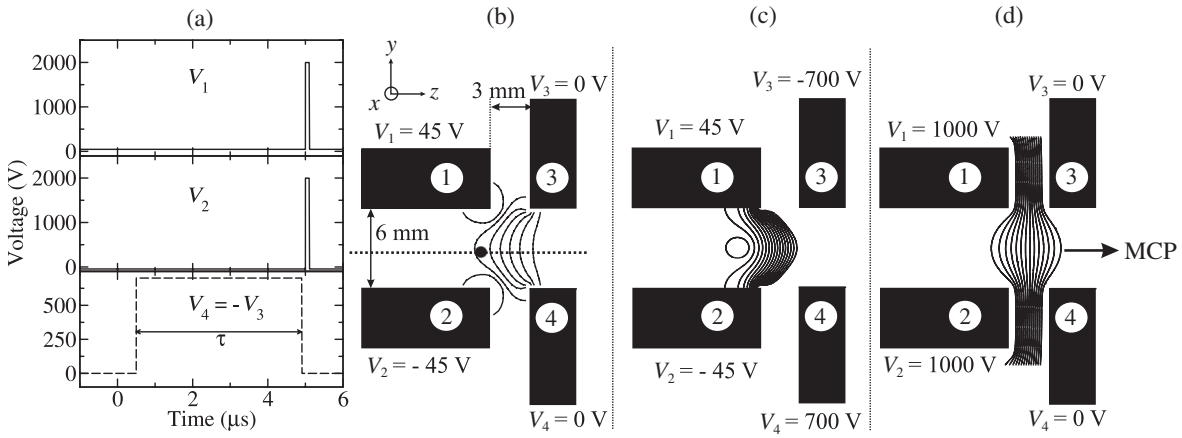

FIG. 1. Panel (a) Voltage sequence used in the mirroring process. Panels (b)–(d) Voltage configurations used to (b) prepare the H atoms in Rydberg Stark states, (c) to reflect the H atoms, and (d) to field ionize the reflected atoms. The width of the electrodes in the x dimension is 2 cm. The solid lines in panels (b), (c) are lines of constant electric field in steps of 25 V/cm (b) and 100 V/cm (c). In panel (d) equipotential lines between 850 V and 200 V in steps of 50 V are shown. The dot in panel (b) marks the photoexcitation point.

low-field seeking character of the Rydberg atoms located in this plane. At positions above or below this plane, the field experienced by the Rydberg atoms does not return to zero at any time during the voltage rise because of the residual component of the field along the z axis. Instead, the direction of the field vector makes an (anti)clockwise rotation for $y > 0$ ($y < 0$). Only a very small (undetectable) fraction of the initially prepared Rydberg atoms are located close enough to the $y = 0$ plane to lose their low-field seeking character; the dipoles of most Rydberg atoms follow the field rotation adiabatically. The electric field strength of ≈ 2000 V/cm between plates 3 and 4 corresponds to a potential energy $E_{\mathrm{Stark}}/hc \approx 50$ cm^{-1} for a $n = 27$, $k = 18$ Stark state. Because the initial kinetic energy of the H atoms is only 21.8 cm^{-1}, they can be stopped and reflected. The potentials on the third and fourth electrodes are switched back to zero after the variable delay τ, just before field ionization. A large field-ionization pulse $V_1 = V_2 = 2000$ V is then applied to plates 1 and 2 to field ionize all Rydberg atoms and extract the ions towards a microchannel plate (MCP) detector where the time-of-flight (TOF) distribution of the ions is monitored. The electric field required to ionize a low-field seeking $n = 27$ Stark state is $\approx$2100 V/cm [5]. The spatial distribution of the ions on the detector can be measured with a CCD camera by taking images of the fluorescence of a phosphor screen connected to the anode of the MCP detector. Both the times of flight and the images of the ions strongly depend on the positions of the parent Rydberg atoms in the electrostatic mirror at the time of field ionization: ion clouds produced close to plates 3 and 4 are subject to a smaller acceleration and have longer times of flight than those produced close to plates 1 and 2. The field distribution [Fig. 1(d)] is such that the former ion clouds expand more than the latter on their way to the detector and form larger images. The images and TOF distributions can therefore be used to reconstruct the position and shape of the Rydberg atom cloud during the mirroring process.

Figure 2(a) shows the TOF distributions obtained after various delays τ between 0.6 μs and 8.6 μs during which $V_4 = -V_3 = 700$ V (solid lines, ''mirror on'' configuration) and $V_4 = -V_3 = 0$ V (dashed lines, ''mirror off''). In the latter case the particles fly through the electrodes with constant velocity and leave the field-ionization region at ≈ 6 μs. The ion times of flight shift to longer times with increasing τ because the voltage difference the ions experience becomes smaller. When the mirror is on ($V_4 = -V_3 = 700$ V) the ion times of flight first increase (by up to 62 ns at $\tau = 3.6$ μs) because the particles move in the forward direction to lower potential. At $\tau = 4.6$ μs, the ion times of flight decrease again, indicating that the Rydberg particles have been reflected and are moving in the backward direction. Panel (b) of Fig. 2 shows a set of simulated ion TOF spectra using the particle trajectory simulation method described in [12]. These simulations do not involve any adjustable parameters but rely on independent measurements of the initial velocity (720 m/s), longitudinal temperature (100 mK), and size of the cloud (FWHM = 0.8 mm). The main deviations between experiment and simulation in Fig. 2 occur at $\tau > 6.6$ μs because in the simulations the particles return to the photoexcitation point slightly earlier than in the experiment. The otherwise good agreement makes us confident that the simulations capture the essential features of the mirror action.

Because the center of the Rydberg cloud at the field-ionization times in the ''mirror off'' experiments can be calculated from the known initial velocity, the TOF spectra can be used to determine where the particles were in the ''mirror on'' experiment. Figure 2(c) compares the position of the center of the atomic cloud at $t_{\mathrm{ion}} = \tau + 500$ ns in the ''mirror off'' and the ''mirror on'' measurements. From the measurements it can be seen that the atomic cloud has

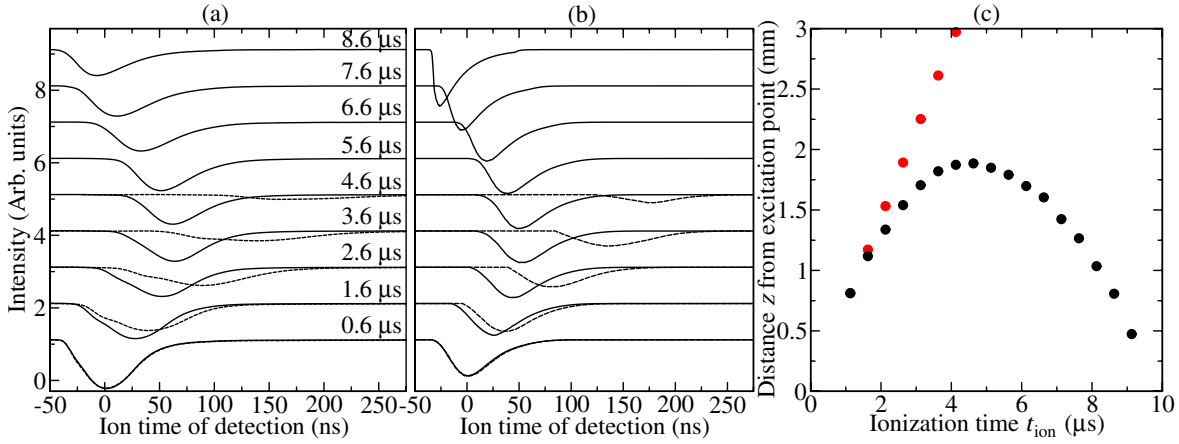

FIG. 2 (color online). Panels (a), (b) TOF distributions of the H^+ ions after deceleration periods τ of (from bottom to top) 0.6 μs, 1.6 μs, 2.6 μs, 3.6 μs, 4.6 μs, 5.6 μs, 6.6 μs, 7.6 μs, and 8.6 μs. The solid lines are measurements with $V_4 = -V_3 = 700$ V and the dashed lines are measurements with $V_4 = -V_3 = 0$ V ("mirror off"). Panel (a) shows the experimental data and panel (b) the simulations. The origin of the time scale is chosen to be at the maximum of the TOF distribution of the $\tau = 0.6$ μs measurement. Panel (c) Comparison between the mirror on and mirror off trajectories of the central part of the atomic cloud. The (red) upper dots show the calculated trajectory of a cloud that moves with a constant velocity of 720 m/s. The (black) lower dots show the measured trajectory of the atomic cloud in the "mirror on" experiments. The dot size is larger than the experimental uncertainty.

come to rest in 4.8 μs only 1.9 mm away from the photoexcitation point and that it has returned to this point after $\approx$9.8 μs.

In panel (a) of Fig. 3, the phase-space distributions in the z dimension are drawn for t_{ion} between 0 and 9 μs. The size of the atomic cloud in the z dimension remains almost constant (FWHM $\approx$ 0.8 mm) during the mirroring process. In the y dimension [panel (b)] the initial particle spread is also 0.8 mm, but the initial velocity is 0 with an effective temperature of only 2.3 mK, leading to a narrow, elongated distribution. The low effective temperature results from skimming the supersonic expansion and from the small vuv spot size [13]. During the mirroring process the particles are accelerated toward the central axis, leading to a narrower particle distribution but a wider velocity spread. In phase space this corresponds to a clockwise rotation of the distribution. At $\approx$6 μs the beam of Rydberg atoms is focused onto the central axis and the temperature in this dimension has risen to 1.2 K. This focusing can also be seen in the simulated particle distributions in the yz plane displayed in Fig. 3(c): after 6 μs the particle density has reached its maximum and after 9 μs the original particle distribution is regained approximately. To exactly reach the original particle distribution, the mirroring time (9.8 μs here) must be equal to half the period of rotation in phase space in the y dimension. In our electrode setup the full period is 24 μs and therefore, although we are close to perfect mirroring, the spatial

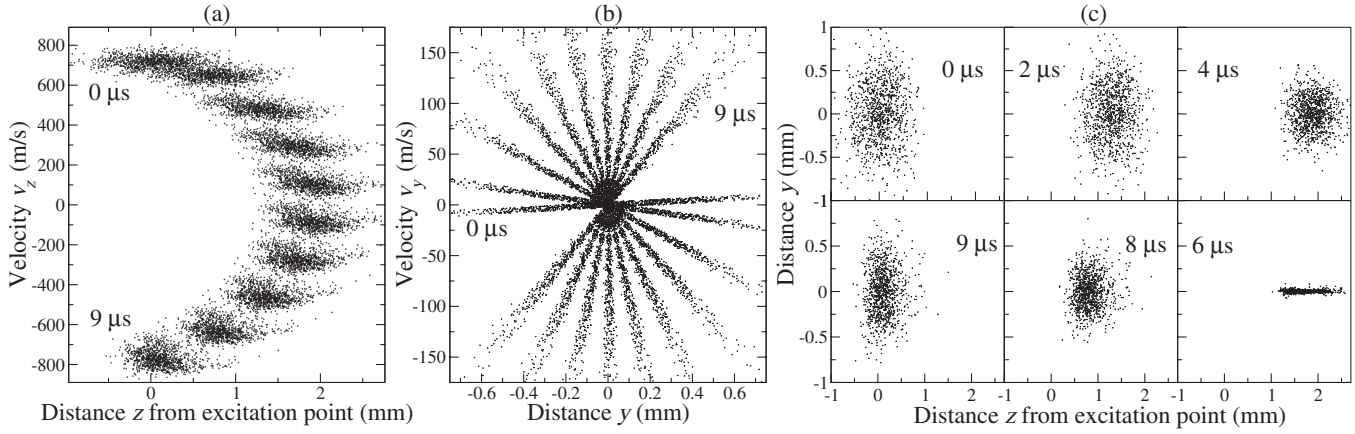

FIG. 3. Panel (a) Simulated phase-space diagrams of the distribution of the Rydberg atom cloud in the z dimension between $t = 0$ (top left corner) and $t = 9$ μs (lower left corner) in steps of 1 μs. Panel (b) Simulated phase-space diagrams in the y dimension at the same times. Panel (c) Simulated distribution of the particles within the electrodes at $t = 0$, 2 μs, 4 μs, 6 μs, 8 μs, and 9 μs. In all these graphs $z = 0$ is the excitation point of the particles.

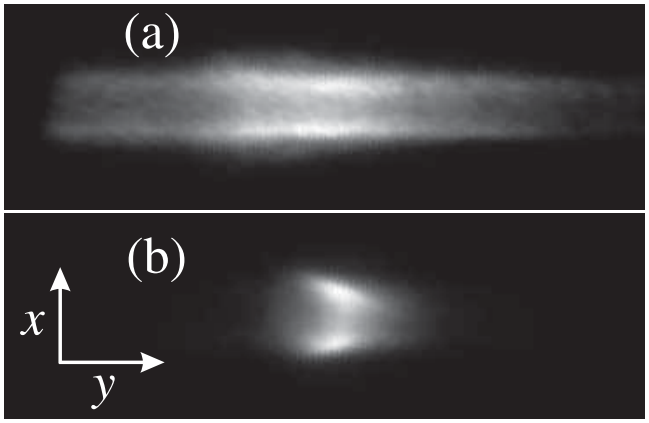

FIG. 4. CCD-camera images of the ions after field ionizing the Rydberg particles in the mirror at (a) $\tau = 2.6$ μs and (b) $\tau = 5.6$ μs. Each image is 25 mm long and 8 mm high. The vuv and uv laser beams propagate along the x axis.

spread in the y dimension is slightly smaller, and the velocity spread slightly wider after reflection.

To verify the predictions of the simulations shown in Fig. 3, CCD-camera images were recorded at different delays τ. Figure 4 displays the observation of the focusing in the y dimension predicted at $t_{\mathrm{ion}} = 6$ μs in panel (c) of Fig. 3. The figure compares images of the Rydberg atom cloud at $\tau = 2.6$ μs, i.e., before focusing [panel (a)] and at $\tau = 5.6$ μs, when the cloud is focused [panel (b)]. The size of the atom cloud is reduced in the y dimension by a factor of more than four at $\tau = 5.6$ μs, as expected from Fig. 3(c). At these 2 times the center of the atom cloud is located at the same point, 1.7 mm away from the photoexcitation spot. One can therefore rule out the possibility that the differences in the images are caused by the dependence of the ion beam divergence on the position of the cloud along the z axis. Both images in Fig. 4 reveal a minimum in the intensity distribution along the $x = 0$ axis. This behavior, which was also observed in images recorded in control experiments carried out in the ''mirror off'' configuration, results from the well-known effect that light gases seeded in heavy gases have the highest density close to the edge of the gas expansion cone [18]. A control measurement in the ''mirror off'' configuration at $t_{\mathrm{ion}} = 2.6$ μs ($\tau = 2.1$ μs), when the center of the cloud is also located 1.7 mm away from the photoexcitation point, yielded images almost identical to that shown in panel (a).

In conclusion, we have demonstrated the mirroring of a Rydberg atom beam at normal incidence. At the end of the mirroring process the atomic cloud has returned to its initial position almost unchanged. Moreover, the phase-space density has remained nearly constant because the decay of the Rydberg Stark states is not significant on the experimental time scale. Using time-of-flight and CCD-camera imaging techniques, we also found that the atomic beam can be focused strongly, leading to a fourfold increase in the particle density, however, at the expense of a wider velocity distribution. These results reveal an unprecedented control over the spatial and velocity distributions of a Rydberg atom cloud. This control is achieved using only small (≤ 2000 V/cm) electric fields and a very compact electrode setup. Halfway through the mirroring process, the atoms are brought back to zero velocity in the laboratory frame after only 4.8 μs and 1.9 mm of flight. Our measurements thus also represent the first direct demonstration that a Rydberg atom beam can be stopped in a single deceleration stage. This study illustrates the advantages of Rydberg states in atom optics experiments and also documents a major step towards another important goal, that of trapping Rydberg atoms in selected Stark states electrostatically.

We thank Dr. S. Willitsch (Oxford) for help with the H atom source. This work is supported by ETH Zurich and the Swiss National Science Foundation.

[1] H. L. Bethlem and G. Meijer, Int. Rev. Phys. Chem. **22**, 73 (2003).
[2] J. Doyle, B. Friedrich, R. V. Krems, and F. Masnou-Seeuws, Eur. Phys. J. D **31**, 149 (2004).
[3] M. R. Tarbutt *et al.*, Phys. Rev. Lett. **92**, 173002 (2004).
[4] D. deMille, Phys. Rev. Lett. **88**, 067901 (2002).
[5] T. F. Gallagher, *Rydberg Atoms* (Cambridge University Press, Cambridge, England, 1994).
[6] T. Seidemann, J. Chem. Phys. **111**, 4397 (1999).
[7] R. J. Gordon, L. Zhu, W. A. Schroeder, and T. Seidemann, J. Appl. Phys. **94**, 669 (2003).
[8] T. Breeden and H. Metcalf, Phys. Rev. Lett. **47**, 1726 (1981).
[9] W. H. Wing, Phys. Rev. Lett. **45**, 631 (1980).
[10] D. Townsend, A. L. Goodgame, S. R. Procter, S. R. Mackenzie, and T. P. Softley, J. Phys. B **34**, 439 (2001).
[11] E. Vliegen, H. J. Wörner, T. P. Softley, and F. Merkt, Phys. Rev. Lett. **92**, 033005 (2004).
[12] E. Vliegen and F. Merkt, J. Phys. B **38**, 1623 (2005).
[13] E. Vliegen, P. A. Limacher, and F. Merkt, Eur. Phys. J. D doi:10.1140/epjd/e2006-00095-1 (2006).
[14] E. Vliegen and F. Merkt, J. Phys. B **39**, L241 (2006).
[15] S. R. Procter, Y. Yamakita, F. Merkt, and T. P. Softley, Chem. Phys. Lett. **374**, 667 (2003).
[16] Y. Yamakita, S. R. Procter, A. L. Goodgame, T. P. Softley, and F. Merkt, J. Chem. Phys. **121**, 1419 (2004).
[17] G. Gabrielse, Adv. At. Mol. Opt. Phys. **50**, 155 (2005).
[18] *Atomic and Molecular Beam Methods* edited by G. Scoles (Oxford University Press, New York, 1988).